Capillary Flows: Dynamics and Geometry Effects

D. Gosselin[*1], J. Berthier[1], D. Chaussy[2] and N. Belgacem[2]

[1]Department of Biotechnology, CEA/Université Grenoble-Alpes, 17 avenue des Martyrs, 38054, Grenoble, France
[2]LGP2, Grenoble-INP Pagora, University of Grenoble, 38402 Saint-Martin d'Hères, France
*Corresponding author: david.gosselin@cea.fr

Abstract: Microfluidic is widely used to create miniaturized and portable devices. Such devices are aimed to constitute diagnostic tools for health monitoring, food industry and environmental monitoring. Considering health care, point-of-care (POC) and home-care devices have been first developed to provide tools for the developing world, but now they are thought to be a universal solution. Such systems are totally autonomous and use capillarity to move fluids. In this work we investigate the dynamics of capillary flows with COMSOL Multiphysics. It is shown that the square root dependency for capillary filling, namely the Lucas-Washburn law for cylindrical ducts, is recovered. Moreover, different geometric configurations such are stop valves and trigger valves have been numerically studied and are presented in this work. Finally, capillary filaments, a.k.a. Concus-Finn filaments, have been numerically investigated by 3D simulations performed in microchannels with sharp inner corners.

Keywords: Capillary flow, Lucas-Washburn law, Stop valve, Trigger valve, Concus-Finn filaments.

1. Introduction

Among the different fields in which microfluidic approach is essential, biotechnological and medical applications are of growing importance [1]. The development of inexpensive and easy-to-use diagnostic tools has been described as an important problem to be addressed by microfluidic [2-3]. Because there are designed for resource-limited sites, these devices should respect some characteristics such as portability, easy handling, user-friendliness and auxiliary equipment independence. These requirements favor capillary solutions which are autonomous and does not require any external power to move the fluid [4-5].

In such systems the knowledge of the flow dynamics is very important to handle properly the samples. The dynamic of capillary flow have been studied since the 1920s for cylindrical channels [6-8]. Studies dealing with non-cylindrical uniform geometries [9-11] have recently been performed. However biological fluids—such as blood—often show non-Newtonian characteristics and modern devices have a more complex geometry than a uniform duct. Thus theoretical studies for these devices may become really complicated and simulations appear as an interesting tool to investigate the behavior of such fluids.

In this work, we show how COMSOL Multiphysics can contribute to the understanding and development of capillary flows.

2. Level-set method with COMSOL Multiphysics

Spontaneous capillary flows (SCF) are studied using the laminar two-phase flow level set method of the COMSOL microfluidic module. This method is used to track a fluid-fluid interface. The governing equations in such study are the Navies-Stokes equations to describe the mass and momentum transport:

$$\nabla \cdot \boldsymbol{u} = 0 \tag{1}$$

$$\rho \frac{\partial \boldsymbol{u}}{\partial t} + \rho(\boldsymbol{u} \cdot \nabla)\boldsymbol{u} = \nabla \cdot [-p\boldsymbol{I} + \mu(\boldsymbol{\nabla u} + (\boldsymbol{\nabla u})^T)] + \boldsymbol{F_{st}} + \rho \boldsymbol{g}) \tag{2}$$

where $\boldsymbol{F_{st}}$ the surface tension force, **u** is the velocity, p is the pressure, μ is the dynamic viscosity and **g** is the gravity vector. An additional equation is the level set equation for the fluid interface:

$$\frac{\partial \phi}{\partial t} + \boldsymbol{u} \cdot \nabla \phi = \gamma \nabla \cdot \left(\epsilon \nabla \phi - \phi \, (1 - \phi) \frac{\nabla \phi}{|\nabla \phi|} \right) \quad (3)$$

where ϕ is the level set function, ϵ is the interface thickness, γ is the re-initialization parameter.

A simple geometry and the flow initial conditions are represented in figure 1. It consists of the channel to be simulated, initially filled with air, and an inlet domain initially filled with water. The wall condition is set to "wetted wall" with a contact angle θ. This contact angle is applied to the fluid 2. Since θ characterizes the contact angle of water, in "properties of fluids" air is the fluid 1 and water the fluid 2.

The inlet boundary has a zero pressure inlet condition and a volumetric fraction of water of 1. The outlet boundary, open to the outside air, has also a zero pressure boundary condition. The boundary between the two initial fluid domains constitutes the initial interface. When it is possible, one can reduce the number of computational meshes by inserting a symmetry condition along the mid-axis.

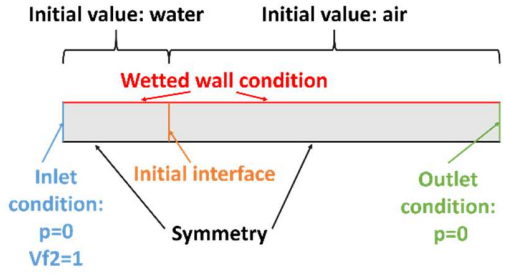

Figure 1. Typical 2D geometry used for simulations of capillary flow along with the boundary conditions.

In this paper, two ways to depict the computational results are used: first, the filling distance as a function of time *z(t)*, second the filling velocity as a function of time *V(t)*. In the first case, the position of the interface at a given time is obtained upon integration of the level set variable along the symmetry line. In the second case, for each time, the filling velocity is obtained by averaging the velocity field on the initial interface.

3. Results and Discussions

Simulations of capillary flows with COMSOL are analyzed from two different aspects. On one hand we have studied the dynamic of capillary filling and more precisely the time dependency of a capillary filling. On the other hand we focused our attention to some geometric effects such a stop valves or Concus-Finn filaments.

3.1 Dynamics of capillary flows.

First the time-dependency of a capillary filling is analyzed. In order to do so, different 2D geometries have been treated using COMSOL. Figure 2 shows the filling distance of a 100µm-wide channel versus time. The contact angle is θ=60°.

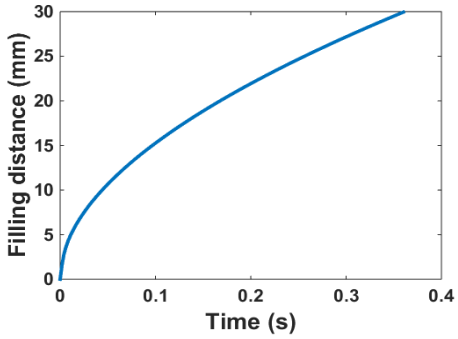

Figure 2. Filling distance versus time for a channel with a width of 100µm and a contact angle of 60°.

A square root dependency of the filling distance according to time is observed, in agreement with the Lucas-Washburn-Rideal (LWR) law [6-8]:

$$z = \sqrt{\frac{r \, \gamma \cos(\theta)}{\mu \, 2}} \sqrt{t} \quad (4)$$

where γ is the surface tension, r is the radius of the capillary tube and θ is the contact angle. Upon derivation of (4), the velocity is expressed by

$$\boldsymbol{u} = \sqrt{\frac{r \, \gamma \cos(\theta)}{\mu \, 8}} \frac{1}{\sqrt{t}} \quad (5)$$

By plotting the filling velocity of the capillary flow versus time (Figure 3), one sees that the dimension of the channel acts as predicted by (5): the smaller the dimensions of the channel, the slower the filling time

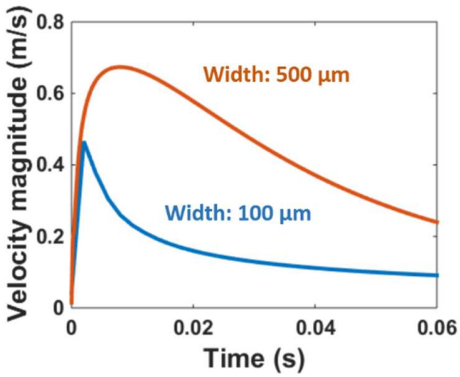

Figure 3. Velocity of the capillary filling time. The smaller the channel, the lower the capillary filling.

In a second step, the capillary filling of a non-uniform channel has been simulated. The geometry consists of narrow and large segments alternately. One observes alternately high and low velocities, according to whether the interface is located in a narrow or large segment, respectively (Figure 4). This is consistent with our recent study and confirmed with experimental observations for a rectangular channels (figure 5).

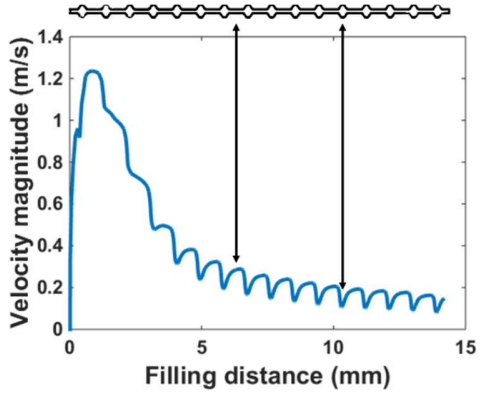

Figure 4. Velocity of the capillary filling versus the filling distance for a non-uniform channel. The geometry of the channel is reminded on top of the plot to link the velocity variations to the geometry variations.

This approach shows that a succession of different dimensions of the channel cross-section complicates the LWR approach of Eq (5). In this particular case, the friction in the narrow sections plays a major role in the dynamics.

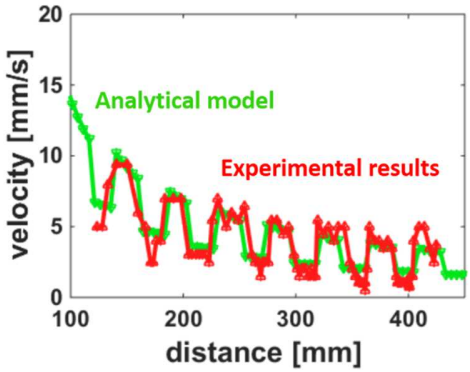

Figure 5. Velocity of the capillary filling for an open rectangle channel for which the width alternates from 300µm to 500µm. The green curve is the analytical model whereas the red curve shows the experimental data.

3.2 Geometrical effects on capillary flows.

In this section, the effects of sudden enlargements of the channel cross-section are analyzed. It is shown that sudden enlargement can act as stop valves, either by pinning the flow on a sharp edge, or simply by a curvature effect [12,13].

Figure 6 shows how the spontaneous capillary flow stops when the interface reaches the enlargement.

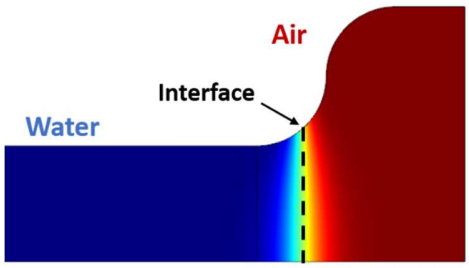

Figure 6. Map of the volume fraction of water within a stop valve when the capillary flow stops. The water is colored in blue, whereas the air is represented in brown. The interface, taken at a volumic fraction of water of 0.5, is depicted with the dashed-line.

As the contact angle with the wall must be θ, the interface flattens when reaching the enlargement, and the Laplace pressure, motor of the capillary

flow, vanishes. Note that the interface thickness plays a major role in such a simulation. In figure 7, one can see that for a thin interface (5µm) the capillary filling is stopped (bright curves) whereas for thick interfaces (darker curves) the capillary filling may pass the enlargement. In fact if the interface is too thick, the flow velocity will decrease at the enlargement but the interface will finally pass through.

Figure 7 also shows that the contact angle has an important effect: in the case of a small contact angle (θ=30°, red curves) the interface appears to pass through the enlargement more easily than in the case of a large contact angle (θ=60°, blue curves). In fact the smaller the contact angle, the thinner must be the interface to be stop by the enlargement. Otherwise it will result in a delay valve and not in a stop valve.

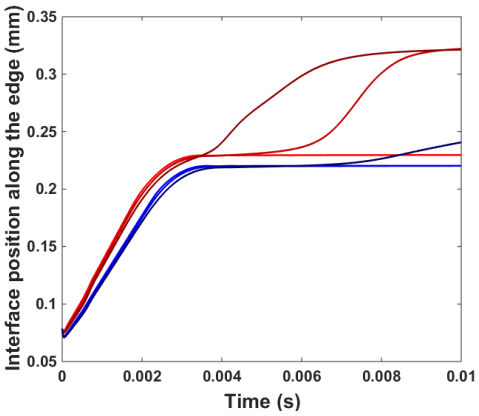

Figure 7. Position of the interface versus time during the capillary filling of the stop valve geometry scheme in Figure 5. Blue curves: contact angle of 60°. Red curves: contact angle of 30°. Different interface thickness have been simulated (from brightest to the darkest: 5, 10 and 20µm).

An elaborated version of the stop valve is the trigger valve shown in figure 8. If a stop valve is located at the wall of a second channel, a flow within this second channel will break the pinning effect and then open the stop valve. Figure 8 shows images from a COMSOL simulation of a trigger valve compared to the experimental pictures. It is observed that the dynamic of the interface for the trigger valve simulated with COMSOL is very consistent with what happens experimentally.

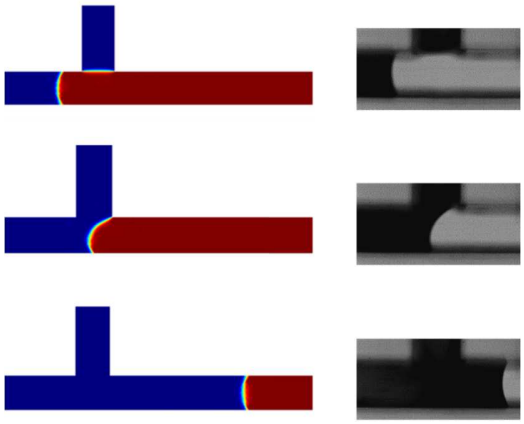

Figure 8. Left: simulation of a trigger valve with COMSOL. Right: Pictures of a trigger valve under capillary flow taken with a high-speed camera.

Finally COMSOL software has also been used to observe a 3D geometric effect: the capillary Concus-Finn filaments [14-16]. This geometry effect occurs inside sharp corners. In such a case no equilibrium position of the interface can be reached and a filament extends endlessly in the corner.

It has been demonstrated that the filament propagates inside the corner, ahead of the main flow, if the following inequality is verified:

$$\theta < \frac{\pi}{2} - \alpha \qquad (6)$$

where θ is the contact angle and α the dihedral half angle.

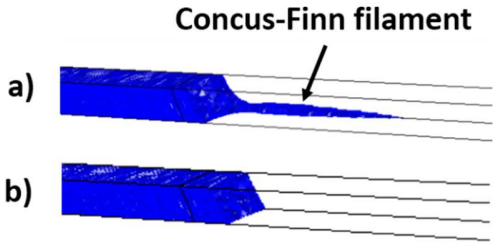

Figure 9. 3D view of a capillary filling within a right angle. In a) the contact angle is 30° (<45°) and there is a Concus-Finn filament, whereas in b) the contact angle is 60° (>45°) and there is no filament.

Figure 9 shows two simulations of a spontaneous capillary flow in a closed rectangular channel (axially cut by two symmetry planes): the first one with a contact angle satisfying (6): $\theta=30°<45°$, and the second one with a contact angle outside inequality (6): $\theta=60°>45°$.

In the first case a filament forms, in the second case there is no precursor filament.

4. Conclusion

In this work, comparisons between known dynamical behaviors of capillary flows and simulations performed with COMSOL Multiphysics have been performed.

First, it is demonstrated that the known $\sqrt{t}$-dependency of a capillary filling (Lucas-Washburn law) is obtain by the simulations. Variation of the filling velocity depending on the dimension of the channel and within non-uniform channels have also been recovered.

On the other hand, geometric effects, i.e. stop and trigger valves, have also been simulated. High-speed camera recording showed that the dynamic of the simulated interface during the trigger is very consistent with experimental experiments.

Finally it is shown that using 3D geometries, Concus-Finn filaments can be obtained along an inner sharp angle if the Concus-Finn relation is verified.

5. References

1. E.K. Sackmann, A.L. Fulton, D.J. Beebe, The present and future role of microfluidics in biomedical research, *Nature*, **507**, 181-189 (2014)

2. G. M. Whitesides, Cool, or simple and cheap? Why not both?, *Lab Chip*, **13**, 11-13 (2013)

3. P. Yager, T. Edwards, E. Fu, K. Helton, K. Nelson, M. R. Tam, B. H. Weigl, Microfluidic diagnostic technologies for global public health, Nature **442** (7101), 412–418 (2006).

4. A. W. Martinez, S.T. Phillips, M. J. Butte, G. M. Whitesides, Patterned Paper as a Plateform for Inexpensive, Low-Volume, Portable Bioassays, *Angew. Chem. Int. Ed*, **46**(8), 1318 (2007)

5. A. W. Martinez, S.T. Phillips, G. M. Whitesides, E. Carrilho, Diagnostics for the developing world: microfluidic paper-based analytical devices, Anal. Chem., **82**, 3-10 (2010).

6. R. Lucas, Ueber das Zeitgesetz des Kapillaren Aufstiegs von Flussigkeiten, *Kolloid Z.*, **23**, 15, (1918)

7. E.W. Washburn, The dynamics of capillary flow, *Phys. Rev*., **17**, 273-283, 1921.

8. E.K. Rideal, On the flow of liquids under capillary pressure, *Philos. Mag*. Ser., **6**(44), 1152-1159 (1922).

9. J. Berthier, K.A. Brakke, E. Berthier, A general condition for spontaneous capillary flow in uniform cross-section microchannels. *Microfluid. Nanofluid*, **16**(4), 779-785 (2014).

10. F. F. Ouali, G. McHale, H. Javed, C. Trabi, N. J. Shirtcliffe, M. I. Newton, Wetting considerations in capillary rise and imbibition in closed square tubes and open rectangular cross-section channels, *Microfluid Nanofluid.*, **15**, 309-326 (2013).

11. J. Berthier and al, A generalization of the Lucas-Washburn-Rideal law to composite microchannels of arbitrary cross-section, *Microfluidics and Nanofluidics*, published on line May 24 (2015).

12. J. Berthier, F. Loe-Mie, V.-M. Tran, S. Schoumacker, F. Mittler, G. Marchand, N. Sarrut, On the pinning of interfaces on micropillar edges, *Journal of Colloid and Interface Science*, **338**, 296–303 (2009).

13. P. Lambert, Surface tension in microsystems: Engineering below the capillary length, Editors: Lambert, Pierre (Ed.), Springer, 2013.

14. P. Concus and R. Finn, On the behavior of a capillary surface in a wedge, *Proceedings of the National Academy of Sciences*, **63**(2), 292–299 (1969).

15. J. Berthier, K. A. Brakke, D. Gosselin, C. Pudda, E. Berthier, Metastable Concus-Finn capillary filaments in rectangular cross- section open microchannels, *AIMS Biophysics*, **1**(1), 31-48 (2014).

16. V. Jokinen, S. Franssila, Capillarity in microfluidic channels with hydrophilic and hydrophobic walls, *Microfluid Nanofluid*, **5**,443–448 (2008).